prosthesis

MDPI

Article

A Novel Reverse Zygomatic Implant Approach: Step-by-Step Protocol and Cadaveric Validation for Trismus and Maxillectomy Sequelae—Part 1

Ada Ferrer-Fuertes [1,2,*], Francisco Javier Cuesta-González [1], Ramón Sieira-Gil [1], Alberto Prats-Galino [2], Samir Aboul-Hosn Centenero [1], Eloy García-Díez [1], Laura Pozuelo-Arquimbau [1], Pau Rodriguez-Berart [1], Irene Vila-Masana [1], Bilal AlOmari [3] and Carles Marti-Pagés [1,*]

1 Maxillofacial Surgery Department, Clinic Hospital, C/Villarroel 170, 08014 Barcelona, Spain; fjcuesta@clinic.cat (F.J.C.-G.); rsieira@clinic.cat (R.S.-G.); saboul@clinic.cat (S.A.-H.C.); emgarcia@clinic.cat (E.G.-D.); lpozueloa@clinic.cat (L.P.-A.); rodriguezs@clinic.cat (P.R.-B.); ivilam@clinic.cat (I.V.-M.)
2 Laboratory of Surgical Neuroanatomy (LSNA), Faculty of Medicine & Health Sciences, Universitat de Barcelona, C/Casanova 143, 08036 Barcelona, Spain; aprats@ub.edu
3 Private Practice, Saudi Society of Periodontology & Implant Dentistry (SSPI), RUMA2742, Riyadh 13249, Saudi Arabia; drbilal.omari@gmail.com
* Correspondence: ferrer@clinic.cat (A.F.-F.); cmarti1@clinic.cat (C.M.-P.)

Abstract

Background: Severe trismus and post-oncologic maxillary defects often prevent conventional zygomatic implant placement. This study evaluates a novel implant specifically designed for reverse insertion (from the zygoma toward the oral cavity) and assesses its feasibility and accuracy in a cadaveric model. **Materials and Methods**: A Brown Class II maxillectomy was simulated in a fresh-frozen cadaver. Four custom reverse zygomatic implants were virtually planned and placed using CAD/CAM surgical guides. Superior and inferior orbital approaches were compared. Postoperative CT was superimposed onto the preoperative plan to measure linear and angular deviations, and a 3D-printed verification bar assessed prosthetic alignment. **Results**: All implants were successfully inserted with primary stability and without compromising critical structures. The superior orbital approach yielded lower deviations and better guide stability, which was reflected in the results: deviation at the zygomatic bone was 1.25 mm in the superior approach vs. 2.32 in the inferior approach, intraorally 4.7 mm vs. 7.3 mm, and angular deviation 1.85° vs. 5.63°. Despite minor distal deflection, intraoral emergence remained within clinically acceptable limits, allowing partial seating of the verification bar. **Conclusions**: Reverse-insertion zygomatic implants are technically feasible, anatomically safe, and compatible with fixed prosthetic rehabilitation in cases where conventional placement is impossible. Penetrating the orbit, injuring the skin or the infraorbital nerve could be possible but guided surgery seems to prevent them. A forthcoming clinical series of eight additional cases will further validate this protocol.

Keywords: zygoma; edentulous mouth; mouth rehabilitation; dental implantation; atrophic maxilla; trismus

Check for updates

Academic Editor: Joseph Nissan

Received: 25 February 2026
Revised: 1 April 2026
Accepted: 10 April 2026
Published: 14 April 2026

Copyright: © 2026 by the authors. Licensee MDPI, Basel, Switzerland. This article is an open access article distributed under the terms and conditions of the Creative Commons Attribution (CC BY) license.

1. Introduction

The loss of teeth has profound functional, social, and psychological consequences. Edentulism has been associated with reduced quality of life, depression, social withdrawal,

and even diminished employment opportunities [1,2]. Dental implant rehabilitation remains the gold standard for replacing missing teeth, restoring both oral function and facial aesthetics. However, successful implant placement requires adequate bone volume to achieve primary stability and long-term osseointegration [1,2].

Zygomatic implants, first described by Brånemark in the 1990s, have revolutionized oral rehabilitation in patients with severe maxillary atrophy [3]. Initially, two posterior zygomatic implants were combined with two to four anterior conventional implants, but subsequent studies demonstrated that full-arch fixed rehabilitation could be achieved using four zygomatic implants alone in cases of advanced maxillary bone loss [4–6]. In less extreme cases, hybrid configurations combining one to three zygomatic implants with conventional implants have been successfully employed to restore dental function [1,7].

Beyond atrophic maxillae, zygomatic implants have also played a crucial role in the reconstruction of patients who have undergone maxillectomy following oncologic resection or trauma, providing stable anchorage for prosthetic rehabilitation even in complex anatomical situations [8]. However, these reconstructive applications are often associated with significant challenges. Soft tissue flaps used to close oncologic defects may lack adequate bone support and can distort normal anatomical landmarks, complicating implant orientation and stability [1]. In addition, post-radiotherapy patients frequently present with trismus, particularly when this is combined with chemotherapy, further limiting mouth opening [1,9]. Given the considerable length of zygomatic implants, adequate mouth opening is essential for conventional insertion. Consequently, these anatomical and functional limitations can preclude the possibility of implant-supported rehabilitation, leaving patients without effective prosthetic solutions for speech, mastication, and aesthetics.

To overcome these anatomical constraints, Dawood et al. [10] reported a pioneering case using zygomatic implants inserted in reverse—that is, from the zygomatic bone toward the oral cavity—achieving successful rehabilitation in a patient with restricted mouth opening. Nevertheless, to the best of our knowledge, the scientific literature lacks further studies exploring this approach or its potential clinical applications.

In this study, we introduce a novel zygomatic implant prototype specifically designed for reverse insertion, together with a detailed description of the surgical protocol. This innovative technique represents a significant advancement in maxillofacial rehabilitation, offering a new treatment alternative for patients with severe trismus or maxillary defects where conventional implant placement is not feasible. By enabling prosthetic restoration in otherwise inoperable cases, this approach could expand the boundaries of implantology and improve the quality of life in a particularly challenging patient population.

2. Materials and Methods

Study Design

A proof-of-concept cadaveric investigation was undertaken to evaluate the technical feasibility, anatomical safety, and positional accuracy of a newly designed reverse-insertion zygomatic implant. The study also aimed to define and validate a standardized surgical protocol for its placement (Figure 1). The experiment was conducted on a fresh-frozen human cadaveric head under laboratory conditions reproducing clinical maxillofacial surgical standards. Ethical approval was obtained from the Ethics Committee of the University of Barcelona (IRB00003099), and all procedures conformed to the ethical principles of the Declaration of Helsinki (2013 revision) and relevant institutional anatomical donation regulations. The experimental setup was designed to simulate a post-maxillectomy scenario with severe posterior maxillary bone loss, similar to those encountered in oncologic reconstruction or advanced atrophic cases (Table 1). The prototype implant was developed

and manufactured by Avinent (Avinent Implant System, Santpedor, Spain) in collaboration with the research team.

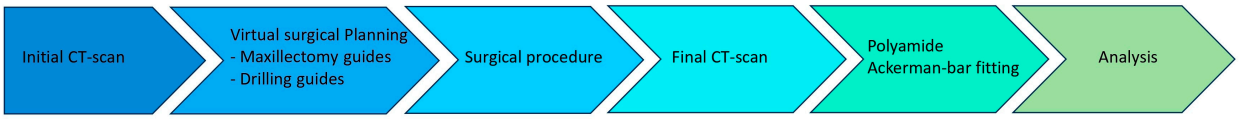


Figure 1. Experimental design of the study.

Table 1. Technique procotol.

1. Initial CT scan and Virtual surgical planning (VSP). 2. Maxillectomy defect with patient-specific CAD/CAM cutting guides, leaving the central incisors as positioning guides. 3. Zygomatic bone approach: • superior blepharoplasty incision with lateral extension • or inferior blepharoplasty incision with lateral canthotomy and cantholysis. 4. Zygomatic bone surface exposure. 5. Polyamide drilling guide adapted to the osseous limits of zygomatic bone and inferior orbital rim. 6. Drilling of the implant path. 7. Implant assembly. 8. Insertion of the implants at a low speed (20–40 rpm). 9. Distal abutment removal, connecting a 30° angled 4.1 × 3 mm transepithelial abutment to the implant body. 10. Final CT scan. 11. Removal of the central incisors. 12. Verification of final intraoral implant position concordance with a custom-shaped polyamide Ackerman-bar over the abutments.

(a) Implant design

The proposed reverse zygomatic implant represents an evolution of the traditional zygomatic concept, specifically engineered to allow retrograde insertion—from the zygomatic body toward the oral cavity—rather than the conventional intraoral-to-zygomatic trajectory.

This orientation was conceived to overcome the anatomical and functional limitations of patients with a restricted oral aperture (trismus), flap reconstructions, or distorted anatomical landmarks, where traditional access routes are impractical or unsafe. Structurally, the implant comprises two integrated but functionally distinct segments:

- Distal non-threaded stem (passive segment)—cylindrical and polished to minimize friction during transzygomatic passage, facilitating atraumatic insertion and reducing heat generation during placement.
- Proximal threaded portion (active segment)—characterized by deep double-threaded spirals with self-tapping cutting edges to achieve bicortical anchorage within the dense zygomatic cortical bone, ensuring primary mechanical stability. The implant diameter ranges from 4.1 mm (passive stem) to 5.0 mm (active threaded portion), and the total length varies from 40 mm to 60 mm, adaptable to the anatomical width and curvature of the zygomatic arch. The threaded portion measures 20 mm and terminates in a universal external hexagonal connection (4.1 mm), which is compatible with standard prosthetic components (Figure 2a).

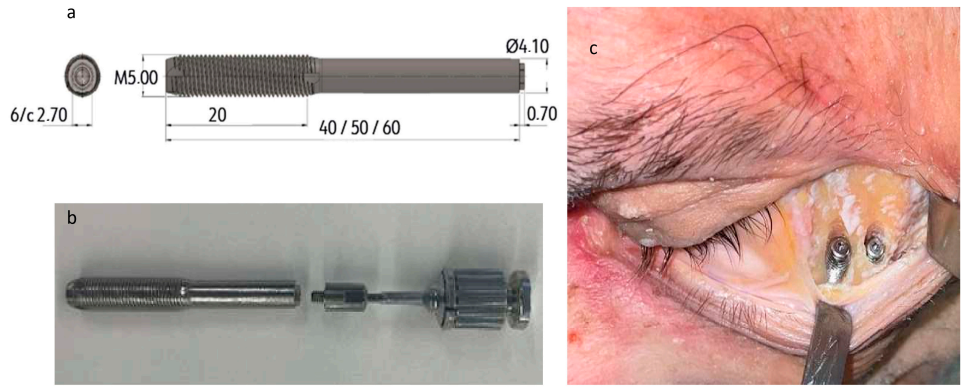


Figure 2. (**a**) Implant design. The threaded end is the proximal end, which remains in the zygomatic bone. The machined end is the distal end, that extends to the mouth. (**b**) Implant (left) with the distal abutment (middle) and the implant screwdriver (right), before assembly. (**c**) Closing cap placed on the zygomatic end of the implant.

The material composition is titanium alloy Grade 23 ELI (Ti6Al4V), chosen for its high fatigue resistance, biocompatibility, and proven osseointegration capacity. A removable external transport carrier is attached to the zygomatic end to enable precise control during insertion and to facilitate orientation (Figure 2b). Once the implant is fully seated, the carrier is removed and replaced by a 30° angled transepithelial abutment connected at the intraoral emergence. The conical transition between the machined passive stem and the threaded active section ensures progressive torque transmission, distributing forces evenly along the zygomatic cortical interface. A sealing screw or cover cap is applied at the zygomatic extremity to prevent soft-tissue ingrowth or contamination within the implant channel (Figure 2c). This feature is essential when the zygomatic surface is covered by reconstructive flaps or dense fibrotic tissue.

(b) Virtual surgical planning

A multiphase virtual planning workflow was implemented to optimize implant trajectory and ensure reproducible placement accuracy. A high-resolution maxillofacial computed tomography (CT) scan was performed with Siemens Somatom Go.Top, 64-slice, VA40A software, 0.6 mm slice thickness(Siemens, Forchheim, Germany). The DICOM datasets were processed using Materialise Mimics Medical 26.0 for segmentation and Materialise 3-Matic Medical 18.0 for three-dimensional planning and design. A Brown Class II maxillectomy defect [11] was digitally simulated to reproduce the clinical scenario of a hemimaxillectomy patient. The four zygomatic implant trajectories were planned to achieve intraoral emergence at the maxillary canine (13, 23) and second premolar (15, 25) regions, thus re-establishing the prosthetic arch and occlusal line.

Each implant was positioned to maximize zygomatic bone contact while avoiding critical structures such as the orbit, infraorbital foramen, zygomaticofacial canal, and temporal fossa. Implant paths were interactively adjusted across multiple planes (axial, sagittal, and coronal) to ensure safe angulation, cortical engagement, and prosthetic emergence alignment. To translate the virtual plan into the cadaveric environment, custom CAD/CAM surgical guides were designed and 3D printed. Two guide systems were manufactured:

a maxillectomy cutting guide to create a reproducible bone defect, and

a zygomatic drilling guide to control implant insertion and angulation.

Both were produced from biocompatible polyamide PA 2200 using a Formiga P110 selective laser sintering printer (EOS GmbH, Krailling, Germany) (Figure 3).

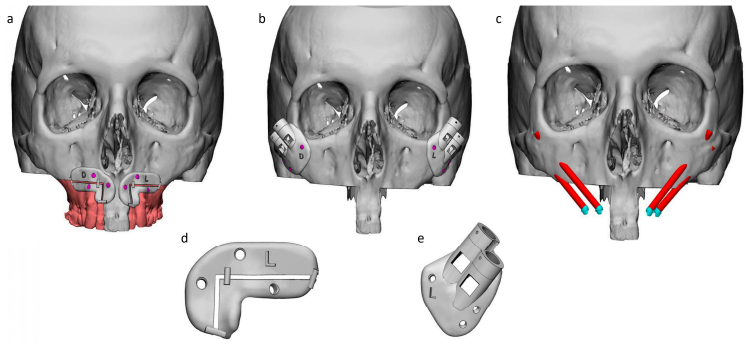


Figure 3. Virtual surgical planning: (**a**) Design of the maxillectomy and the polyamide cutting guides. (**b**) Design of the drilling guides for implant placement and their positioning over the zygomatic bone. (**c**) Planned position of the implants. (**d**) Left cutting guide for maxillectomy. (**e**) Left drilling guide for implant placement.

(c) Surgical protocol

All procedures were conducted under continuous irrigation with saline (0.9% sodium chloride) to prevent overheating of the cortical bone. The virtual plan and 3D guide reference images were continuously displayed during surgery to ensure adherence to the pre-planned trajectories.

- Step 1. Maxillectomy and anatomical exposure
  A Class II maxillectomy was executed intraorally following the CAD/CAM cutting guide (Figure 3a,e), stabilized with three titanium screws (Titamed, Kontich, Belgium). The central incisors were retained as positional references for later prosthetic alignment. Subsequently, bilateral orbital approaches were tested to evaluate surgical access and visibility of the zygomatic bone:
  - On the right side, a superior blepharoplasty incision with lateral extension was performed (Figure 4a).
  - On the left side, an inferior blepharoplasty with lateral canthotomy and cantholysis was used (Figure 4b). Both approaches enabled full exposure of the zygomatic body, lateral and inferior orbital rims, infraorbital nerve, zygomaticotemporal suture, and frontal process of the zygoma.

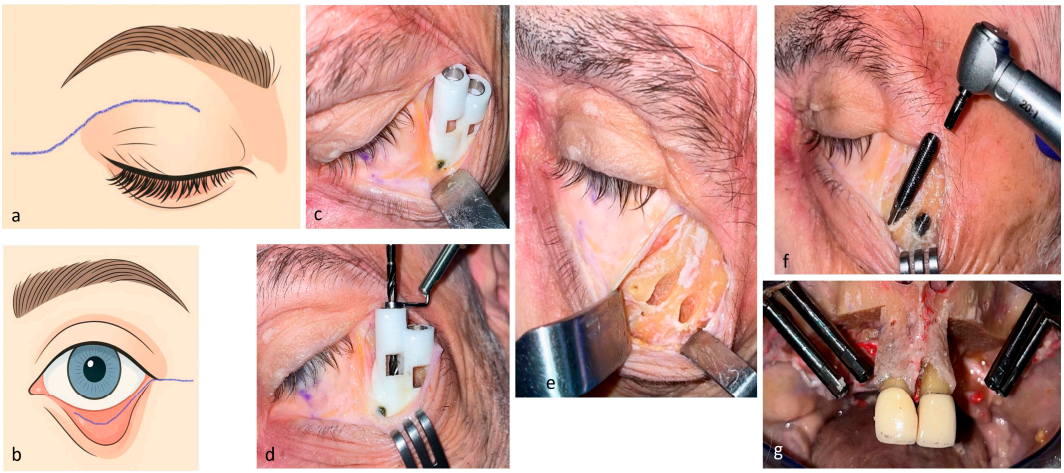


Figure 4. (**a**) Right superior blepharoplasty incision. (**b**) Left inferior blepharoplasty incision with cantholysis. (**c**) Drilling guide in the inferior blepharoplasty approach. (**d**) Drilling procedure. (**e**) Implant paths on the left zygomatic bone. (**f**) Implant placement. (**g**) Intraoral emergence of the implants.

- Step 2. Drilling sequence
  The polyamide drilling guide (Figures 3b,e and 4c) was adapted to the zygomatic contour and secured with three titanium screws. A temporal support flange ensured proper spatial orientation. Sequential drilling was performed, using removable internal metal sleeves and standard zygomatic implant burs: Southern Implants (Irene, South Africa), Straumann (Basel, Switzerland), Avinent (Santpedor, Spain) with low-speed, high-torque settings under copious saline irrigation (Figure 4d). Drilling was performed progressively until full transzygomatic penetration was achieved, ensuring that the exit point coincided with the previously planned intraoral emergence site.
- Step 3. Implant insertion
  Before placement, each implant was assembled with a distal protective carrier to safeguard the prosthetic interface during manipulation (Figure 2b). Implants were inserted in a reverse orientation, progressing from the zygomatic surface toward the oral cavity, at a rotational speed of 20–40 rpm and a torque of 40 N·cm (Figure 4f). Final seating was achieved manually, ensuring intimate cortical engagement without microfracture. Following full insertion, the carrier was detached, and a 30° angled 4.1 × 3 mm transepithelial abutment (Avinent, Santpedor, Spain) was attached (Figure 2c). The abutments were oriented to achieve parallelism and to simulate optimal prosthetic alignment. All surgical steps were documented through intraoperative photography and high-definition videography for procedural validation and reproducibility.

(d) Postoperative assessment and 3D analysis

Upon implant placement, linear anatomical measurements were performed directly on the specimen to evaluate spatial relationships, including:

- The distance between the most anterior implants and the vertical osteotomy line of the premaxilla (Figure 5a).
- Linear inter-implant distances within each hemiarch (Figure 5b).

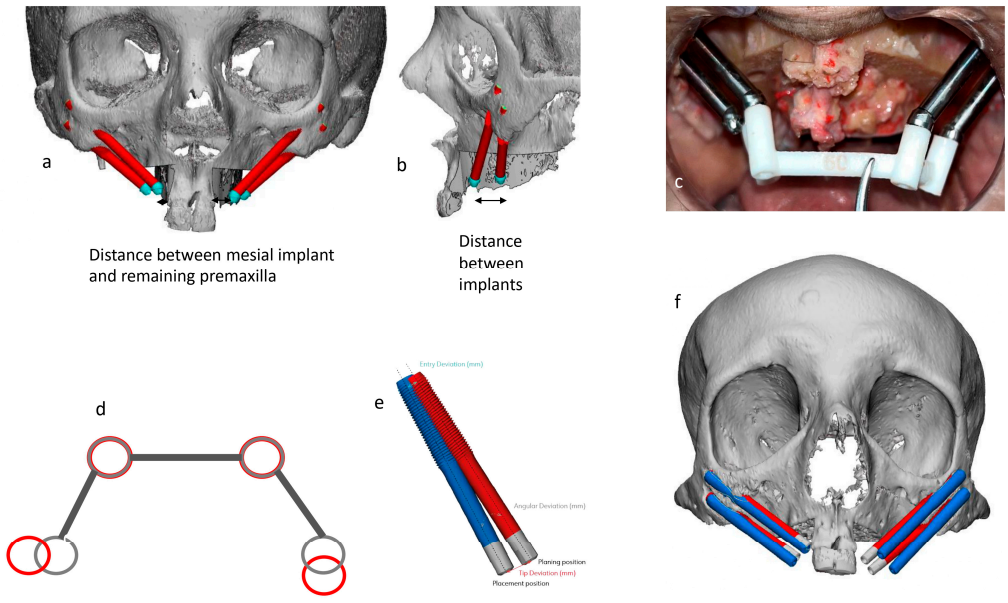


Figure 5. Intraoral measurements: (**a**) From the medial implant to the vertical premaxilla osteotomy. (**b**) Between the anterior and posterior implants. (**c**) Frontal view of emergence concordance between the multiunit abutments and the polyamide bar simulating an Ackerman-bar. (**d**) Occlusal view of emergence concordance between the multiunit abutments and the polyamide bar simulating an Ackerman-bar. (**e**) Linear and angular deviations were measured compared to the axis of the implants. (**f**) Comparison between the planned surgery (red) and the final result (blue).

A postoperative CT scan was acquired using the same scanner parameters to allow 3D superimposition onto the preoperative plan. The central incisors were retained to facilitate alignment between both DICOM datasets. A custom-designed polyamide verification bar mimicking an Ackerman-type prosthetic bar was fabricated according to the planned intraoral emergence points. The bar was fitted, after removing the incisors, onto the abutments to verify prosthetic passivity and spatial correspondence between planned and achieved positions (Figure 5c,d).

Subsequent 3D reconstruction and comparison analyses were carried out using Materialise Mimics Medical 26.0 and 3-Matic Medical 18.0 software. Quantitative assessments included:

- Linear deviation (mm) at the zygomatic and intraoral entry/exit points (Figure 5f).
- Angular deviation (°) between the planned and actual implant axes (Figure 5e,f).
- Zygomatic bone volume (mm^3).

These data allowed for precise validation of the surgical accuracy, biomechanical stability potential, and reproducibility of the reverse insertion technique.

(e) Outcome parameters

Primary outcome measures were:

- Feasibility of reverse implant placement through zygomatic bone without cortical perforation or involvement of anatomical structures such as the orbit, temporal fossa, infraorbital nerve or the skin.
- Accuracy of placement compared with the virtual plan.
- Accessibility and visibility differences between the superior and inferior orbital approaches.

Secondary outcomes included the assessment of the prosthetic alignment feasibility and absence of iatrogenic risk to adjacent structures such as the orbit, infraorbital nerve, and temporal fossa.

3. Results

A proof-of-concept cadaveric experiment was successfully performed using static guided surgery to evaluate the feasibility and accuracy of the reverse-insertion zygomatic implant protocol. Four prototype implants were placed bilaterally in the maxilla of a fresh-frozen cadaveric specimen according to the preoperative virtual plan. All implant sites were prepared using patient-specific 3D-printed drilling guides designed from the virtual surgical simulation.

3.1. Surgical Feasibility and Intraoperative Performance

Both orbital access approaches—the right superior blepharoplasty with lateral extension and the left inferior transconjunctival blepharoplasty with lateral canthotomy and cantholysis—provided excellent exposure of the zygomatic body, lateral orbital rim, and infraorbital region. This exposure allowed stable and reproducible positioning of the polyamide drilling guides without mechanical interference or deformation.

Soft-tissue management was crucial to prevent tension or obstruction from the buccal fat pad and malar soft tissues. When these were adequately retracted, implant insertion was smooth and ergonomically feasible, with no conflict with adjacent anatomical structures such as the orbital floor, zygomatic arch, or temporal fossa.

All four implants reached full seating without mechanical complications. Primary stability was achieved in all cases, confirmed by manual torque control and absence of micromovement. A slight elastic flexion was noted near the intraoral (occlusal) end during placement, likely related to the long, narrow stem traversing the zygomatic canal, but it did not compromise anchorage or abutment alignment.

3.2. Zygomatic Bone Anatomy and Implant Distribution

The zygomatic bone volumes were measured at 4.08 cm^3 on the right side and 4.65 cm^3 on the left side, providing sufficient cortical density for stable anchorage (Table 2).

Table 2. Deviations regarding planned and postoperative results.

	Right		Left	
Implant Position	13	15	23	25
Zygomatic Bone Volume (cm^3)	4.08		4.65	
Implant Length (mm)	50	40	50	40
COMPARISON OF IMPLANT POSITION				
Lineal deviation at zygomatic bone (mm)	0.9	1.6	3.77	5.64
Lineal intraoral deviation (mm)	1.23	3.41	6.46	8.14
Angular deviation (°)	0.65	3.04	4.29	6.96
Angle regarding vertical line (°)	43.41	44.59	33.96	37.61
% implant outside the bone	68.22%	79.96%	78.51%	79.62%
Matching with polyamide bar *	+++	+	+++	+

* Degree of concordance was assessed by visual inspection. +++ indicates full concordance, + indicates approximately one third.

Implant dimensions were adapted to the virtual plan:

- Anterior implants (positions 13 and 23): 50 mm length.
- Posterior implants (positions 15 and 25): 40 mm length (Table 2).

Linear intraoral measurements confirmed anatomical symmetry between both sides, with 9 mm between implants 13 and 15, and 15 mm between implants 23 and 25. The distance from the right anterior implant (13) to the premaxillary osteotomy was 3 mm, and from the left anterior implant (23) to its corresponding osteotomy line was 11 mm (Table 3).

Table 3. Linear measurements.

	Linear Measurements					
	Distance Between Implants at Zygomatic Bone (mm)		Distance from Mesial Implant to Premaxilla Osteotomy (mm)		Intraoral Distance Between Mesial and Distal Implants (mm)	
	Right	Left	Right	Left	Right	Left
Intraoral	-	-	3	11	9	15
Preoperative CT	8.9	8.8	1.73	5.42	9.38	10.54
Postoperative CT	9.56	7.62	1.75	10.22	8.67	14.13
Differences in preoperative–postoperative CT	0.02	1.12	0.02	4.8	0.71	3.59

3.3. Accuracy Analysis: Comparison Between Planned and Achieved Positions

A postoperative CT scan was acquired and digitally superimposed onto the virtual plan to assess linear and angular deviations.

Deviations were measured at two reference points for each implant:

1. The zygomatic entry point (proximal segment).
2. The intraoral emergence (distal segment).

Additionally, the angular deviation between the planned and actual implant axes was computed.

Results demonstrated that linear deviation was consistently greater at the intraoral emergence, indicating minor deflection during the long transzygomatic path. The smallest overall deviation occurred at position 13 (1.23 mm), while the greatest was observed at position 25 (8.14 mm) (Table 2).

Mean deviations were significantly smaller on the right side (1.23 mm and 3.41 mm) than on the left side (6.46 mm and 8.14 mm), correlating with better mechanical control in the superior blepharoplasty approach. This difference suggests that the superior orbital access provides enhanced drill stability and depth control compared with the inferior approach, but it could also be attributed to suboptimal placement of the drilling guide.

Angular deviations followed a similar pattern, being minimal on the right side and greater on the left, where implant trajectories showed less inclination relative to the vertical axis (Table 3). The observed angular variance likely reflects minor intraoperative guide movement during the inferior blepharoplasty procedure, where soft-tissue elasticity and surgical ergonomics are more challenging, or potentially inaccurate positioning of the guide.

3.4. Prosthetic Alignment and Intraoral Verification

After placement, the polyamide verification bar was placed over the multi-unit transepithelial abutments to assess intraoral alignment accuracy and prosthetic feasibility (Figure 5c).

The two anterior implants (positions 13 and 23) exhibited complete passivity and perfect alignment with the predesigned bar, confirming accurate correspondence with the virtual plan. In contrast, the two posterior implants (positions 15 and 25) achieved only partial contact (approximately one-third of the bar width), reflecting minor distal deflection consistent with the CT-measured deviations (Table 3).

Despite these discrepancies, the overall intraoral emergence pattern remained within clinically acceptable limits for prosthetic restoration. The prosthetic space and angulation of all four abutments were sufficient to allow the fabrication of a fixed dental prosthesis without mechanical interference or excessive divergence.

3.5. Overall Findings and Procedural Validation

The experimental outcomes confirmed that the reverse-insertion zygomatic implant concept is surgically feasible, anatomically safe, and mechanically stable.

No perforation of the orbital floor, maxillary sinus, or infratemporal fossa was detected. The guided surgical system allowed accurate transzygomatic drilling and implant positioning, with deviations comparable to those reported in conventional zygomatic guided implantology (<2 mm at the entry point, <8 mm at the exit point, and <5° angular variance).

The superior blepharoplasty approach appeared to offer superior control, reduced angular deviation, and better visibility compared with the inferior orbital access. Both approaches, however, provided adequate exposure and allowed safe manipulation of the instruments.

Finally, prosthetic verification confirmed that intraoral emergence alignment was sufficiently precise to support an immediate or delayed prosthesis, validating the potential clinical translatability of this reverse-insertion protocol for patients with restricted oral access or extensive maxillary defects.

4. Discussion

This proof-of-concept cadaveric study demonstrates, for the first time, the feasibility, safety, and positional accuracy of a newly designed zygomatic implant conceived specifically for reverse insertion. This approach directly addresses the clinical limitations described in the introduction—namely, severe trismus, altered maxillary anatomy due to oncologic resections, and restricted intraoral access—which often preclude placement of conventional zygomatic implants [1,9]. The present findings expand upon the isolated case described by Dawood et al. (2015) [10], offering the first structured design rationale and standardized surgical protocol for reverse-trajectory zygomatic implant placement.

In their study, Dawood et al. only placed one reverse zygomatic implant on one side affected by hemimaxillectomy, combining it with two conventional zygomatic implants on the other side. This approach would not address the problem of the limited mouth opening. Furthermore, no data was provided regarding differences in accuracy between planification and final result.

The implant's dual-segment configuration—passive polished transzygomatic stem and active 20-mm threaded engagement portion—was validated as compatible with zygomatic bone anatomy. Previous analyses report intra-malar bone lengths rarely exceeding 20 mm [12], supporting the chosen active-thread length. The 5.0-mm thread diameter was dimensioned to enhance cortical anchorage, consistent with mechanical principles described for conventional zygomatic implants [13]. The reverse orientation does not rely on crestal bone as a reference, which is advantageous in post-maxillectomy cases where such landmarks are absent.

Both orbital approaches tested provided adequate access; however, the superior blepharoplasty incision yielded smaller linear and angular deviations, correlating with improved drill stability and guide adaptation. This aligns with previous anatomical descriptions of supratarsal access, which emphasize predictable exposure of the zygomatic body and temporal buttress [14–16]. In contrast, the inferior transconjunctival approach, although effective, may be more vulnerable to soft-tissue elasticity and guide mobility, partially explaining the deviations observed [17,18]. The polyamide guides could also be applied to living patients, as used in other maxillofacial surgeries. Beyond the widespread use of polyamide, other polymers suitable for surgical guides are PMMA, valued for its translucency and low cost, and PEEK, characterized by its enhanced mechanical properties [19]. However, accuracy could be improved if surgery were assisted by navigation (dynamic computer-aided surgery), to ensure perfect guide and implant placement.

The magnitude and pattern of deviations observed—minimal at the zygomatic entry and greater at the long transzygomatic trajectory—are consistent with inaccuracies reported in guided zygomatic implantology (<2 mm entry, <8 mm exit, <5° angulation) [20]. Although deviations were higher on the left side, possibly due to guide mispositioning, prosthetic verification demonstrated that intraoral emergence remained within clinically acceptable limits.

The intraoral verification bar confirmed precise alignment for the anterior implants and partial, yet acceptable, alignment for posterior implants. Literature suggests that long-term stability in quadruple-zygoma frameworks depends largely on splinting and anterior implant load distribution [8–13]. Given that reverse zygomatic implants transfer occlusal forces directly to the zygoma in the absence of alveolar support, the posterior pair is likely to experience the highest mechanical stresses [21]. While increasing implant diameter could theoretically reduce fracture risk [22], anatomical constraints may limit such modifications in certain patients.

Recent advances in subperiosteal implants and ZIP-flap reconstructions provide valid alternatives for maxillary rehabilitation [23–26]. However, these methods often require

immediate planning at the time of oncologic surgery or the presence of vascularized bone flaps. For patients reconstructed solely with soft-tissue flaps—or those who underwent maxillectomy years earlier—the reverse-insertion implant may offer a more straightforward and less invasive route to fixed dental rehabilitation.

This study provides a reproducible surgical protocol supported by CT-based planning, CAD/CAM drilling guides, and quantitative 3D accuracy assessments. However, several inherent limitations exist. Cadaveric heads cannot model functional trismus, dynamic soft-tissue behavior, or prosthodontic constraints related to reduced oral aperture. Additionally, although intraoral emergence proved satisfactory for bar fitting, full prosthesis fabrication was not performed.

As the sample is small, conclusions about clinical applicability remain preliminary. Further validation in clinical series is required to determine the feasibility of the different approaches and possible technical difficulties during surgery, as well as long-term biomechanical behavior, prosthetic performance, and complication rates. In the long term, deviations in intraoral emergence may lead to poorer hygiene and consequently peri-implant leakage, bulky prostheses, material fatigue and possible difficulty in speech.

The research team is currently preparing a subsequent article that will include eight additional clinical cases treated with this same protocol, which will provide essential clinical and functional outcome data. It is expected that accuracy will tend toward deviations around 1–3 mm and less than 5°.

If this further research confirmed satisfactory results, it could be introduced to clinical practice and help patients without alternatives for oral rehabilitation.

5. Conclusions

In summary, this study introduces and validates a novel reverse-insertion zygomatic implant system and surgical workflow. The proposed technique overcomes key anatomical and functional limitations in patients with severe trismus or maxillary defects, offering a promising alternative for fixed rehabilitation in cases where conventional zygomatic implants are not feasible. Future clinical studies with larger cohorts will be essential to assess long-term precision, stability, and clinical outcomes.

Author Contributions: Conceptualization, A.F.-F. and C.M.-P.; methodology, A.F.-F. and C.M.-P.; formal analysis, A.F.-F. and C.M.-P.; validation, A.F.-F. and C.M.-P.; software, A.F.-F. and C.M.-P.; investigation, A.F.-F. and C.M.-P.; resources, A.F.-F. and C.M.-P.; data curation, A.F.-F.; writing—original draft preparation, A.F.-F. and C.M.-P.; writing—review and editing, F.J.C.-G., A.P.-G., R.S.-G., S.A.-H.C., E.G.-D., L.P.-A., P.R.-B., I.V.-M. and B.A.; visualization, A.F.-F.; supervision, C.M.-P.; project administration, C.M.-P.; funding acquisition, C.M.-P. All authors have read and agreed to the published version of the manuscript.

Funding: This research received no external funding.

Institutional Review Board Statement: This study was conducted on a fresh-frozen human cadaveric head under laboratory conditions reproducing clinical maxillofacial surgery standards. Ethical approval was obtained from the Ethics Committee of the University of Barcelona (IRB00003099, date of approval: 28 February 2022), and all procedures conformed to the ethical principles of the Declaration of Helsinki (2013 revision) and relevant institutional anatomical donation regulations.

Informed Consent Statement: Patient consent was waived for this study as the cadaveric specimen used was provided by the University's Anatomy Laboratory. The donor had expressly bequeathed their body pre-mortem, signing an informed consent form that permits its use for both educational and research purposes.

Data Availability Statement: All data supporting the reported results can be found in the article (Tables 2 and 3).

Acknowledgments: The authors would like to thank Avinent for their technical support and for providing the materials necessary develop the project. During the preparation of this manuscript/study, the authors used Chat GPT5.2 for the purposes of drawing the incisions used in the study (Figure 4a,b). The authors have reviewed and edited the output and take full responsibility for the content of this publication.

Conflicts of Interest: Avinent (Santpedor, Spain) provided materials and collaborated on surgical planning and the subsequent comparison of planned versus clinical outcomes. The funders played no role in the study design; the collection, analysis, or interpretation of data; the drafting of the manuscript; or the decision to publish the results. No financial compensation was exchanged between the funders and the authors. The remaining authors declare no conflicts of interest.

References

1. Shirota, T.; Shimodaira, O.; Matsui, Y.; Hatori, M.; Shintani, S. Zygoma implant-supported prosthetic rehabilitation of a patient with a maxillary defect. *Int. J. Oral Maxillofac. Surg.* **2011**, *40*, 113–117. [CrossRef]
2. Hao, Y.; Yuan, Z.; Zhu, Y.; Li, S.; Gou, J.; Dong, S.; Niu, L. Association between tooth loss and depression mediated by lifestyle and Inflammation-a cross-sectional investigation. *BMC Public Health* **2024**, *24*, 2627. [CrossRef] [PubMed]
3. Brånemark, P.I.; Gröndahl, K.; Ohrnell, L.O.; Nilsson, P.; Petruson, B.; Svensson, B.; Engstrand, P.; Nannmark, U. Zygoma fixture in the management of advanced atrophy of the maxilla: Technique and long-term results. *Scand. J. Plast. Reconstr. Surg. Hand. Surg.* **2004**, *38*, 70–85. [CrossRef] [PubMed]
4. Balshi, T.; Wolfinger, G.J.; Petropoulos, V.C. Quadruple zygomatic implant support for retreatment of resorbed iliac crest bone graft transplant. *Implant Dent.* **2003**, *12*, 47–53. [CrossRef]
5. Bothur, S.; Jonsson, G.; Sandahl, L. Modified technique using multiple zygomatic implants in reconstruction of the atrophic maxilla: A technical note. *J. Oral Maxillofac. Implant.* **2003**, *18*, 902–904.
6. Aboul-Hosn Centenero, S.; Lázaro, A.; Giralt-Hernando, M.; Hernández-Alfaro, F. Zygoma Quad Compared With 2 Zygomatic Implants: A Systematic Review and Meta-analysis. *Implant Dent.* **2018**, *27*, 246–253. [CrossRef]
7. Pellegrino, G.; Tarsitano, A.; Basile, F.; Pizzigallo, A.; Marchetti, C. Computer-Aided Rehabilitation of Maxillary Oncological Defects Using Zygomatic Implants: A Defect-Based Classification. *J. Oral Maxillofac. Surg.* **2015**, *73*, 2446.e1–2446.e11. [CrossRef]
8. Vosselman, N.; Glas, H.H.; Merema, B.J.; Kraeima, J.; Reintsema, H.; Raghoebar, G.M.; Witjes, M.J.H.; de Visscher, S.A.H.J. Three-Dimensional Guided Zygomatic Implant Placement after Maxillectomy. *J. Pers. Med.* **2022**, *12*, 588. [CrossRef]
9. Borges, M.M.; Malta, C.E.; Ribeiro, R.S.; Cetira-Filho, E.L.; de Moura, J.F.; Rebouças, L.M.; Costa, F.W.; Silva, P.B.; Mota, M.R. Chemotherapy increases the prevalence of radiotherapy-related trismus in head and neck cancer patients: A systematic review and meta-analysis. *J. Clin. Exp. Dent.* **2024**, *16*, e503–e515. [CrossRef]
10. Dawood, A.; Collier, J.; Darwood, A.; Tanner, S. The reverse zygomatic implant: A new implant for maxillofacial reconstruction. *Int. J. Oral Maxillofac. Implant.* **2015**, *30*, 1405–1408. [CrossRef] [PubMed]
11. Brown, J.S.; Rogers, S.N.; McNally, D.N.; Boyle, M. A modified classification for the maxillectomy defect. *Head Neck* **2020**, *22*, 7–26. [CrossRef]
12. Bertos Quílez, J.; Guijarro-Martínez, R.; Aboul-Hosn Centenero, S.; Hernández-Alfaro, F. Virtual quad zygoma implant placement using cone beam computed tomography: Sufficiency of malar bone volume, intraosseous implant length, and relationship to the sinus according to the degree of alveolar bone atrophy. *Int. J. Oral Maxillofac. Surg.* **2017**, *47*, 252–261. [CrossRef]
13. Bedrossian, E.; Bedrossian, E.A. Prevention and the Management of Complications Using the Zygoma Implant: A Review and Clinical Experiences. *Int. J. Oral Maxillofac. Implant.* **2023**, *33*, e135–e145. [CrossRef]
14. Kung, D.S.; Kaban, L.B. Supratarsal fold incision for approach to the superior lateral orbit. *Oral Surg. Oral Med. Oral Pathol. Oral Radiol. Endod.* **2016**, *81*, 522–525. [CrossRef] [PubMed]
15. Abussuud, Z.; Ahmed, S.; Paluzzi, A. Surgical Approaches to the Orbit: A Neurosurgical Perspective. *J. Neurol. Surg. B Skull Base* **2020**, *81*, 385–408. [CrossRef]
16. Das, D.; Modaboyina, S.; Gupta, S.; Deora, A.; Agrawal, S. Surgical approaches to the orbit—The past and the present. *IP Int. J. Ocul. Oncol. Oculoplasty* **2021**, *7*, 5–11. [CrossRef]
17. Uemura, T.; Watanabe, H.; Masumoto, K.; Chuman, T.; Satake, Y.; Yanai, T.; Harada, Y.; Ishihara, Y.; Kikuchi, M. Transconjunctival Approach for Zygomatic Fracture: A Single Surgeon's Experience of More Than 20 Years. *Plast. Reconstr. Surg. Glob. Open* **2016**, *4*, e757. [CrossRef]
18. Mombaerts, I.; Allen, R.C. The transconjunctival orbitotomy: A versatile approach to the orbit and beyond. *Surv. Ophthalmol.* **2023**, *68*, 265–279. [CrossRef] [PubMed]
19. Lepišová, M.; Tomášik, J.; Oravcová, Ľ.; Thurzo, A. Three-Dimensional-Printed Elements Based on Polymer and Composite Materials in Dentistry: A Narrative Review. *Bratisl. Med. J.* **2025**, *126*, 14–27. [CrossRef]

20. Vercruyssen, M.; Cox, C.; Coucke, W.; Naert, I.; Jacobs, R.; Quirynen, M. A Randomized Clinical Trial Comparing Guided Implant Surgery (Bone- or Mucosa-Supported) With Mental Navigation or the Use of a Pilot-Drill Template. *J. Clin. Periodontol.* **2014**, *41*, 717–723. [CrossRef]
21. Tezerişener Özalp, Ö.; Altay, M.A.; Sindel, A. Comparison of stress distribution around all-on-four implants of different angulations and zygoma implants: A 7-model finite element analysis. *BMC Oral Health* **2024**, *24*, 176. [CrossRef]
22. Korkmaz, F.M.; Korkmaz, Y.T.; Yaluğ, S.; Korkmaz, T. Impact of dental and zygomatic implants on stress distribution in maxillary defects: A 3-dimensional finite element analysis study. *J. Oral Implantol.* **2012**, *38*, 557–567. [CrossRef]
23. Mommaerts, M.Y. Additively manufactured sub-periosteal jaw implants. *Int. J. Oral Maxillofac. Surg.* **2017**, *46*, 938–940. [CrossRef] [PubMed]
24. Butterworth, C.J.; Lowe, D.; Rogers, S.N. The Zygomatic Implant Perforated (ZIP) flap reconstructive technique for the management of low-level maxillary malignancy—Clinical patient related outcomes on 35 consecutively treated patients. *Head Neck* **2022**, *44*, 345–358. [CrossRef] [PubMed]
25. Gellrich, N.C.; Rahlf, B.; Zimmerer, R.; Pott, P.C.; Rana, M. A new concept for implant-borne dental rehabilitation; how to overcome the biological weak-spot of conventional dental implants? *Head Face Med.* **2024**, *13*, 17. [CrossRef]
26. McMillan, D.C.; McMillan, K.B.; Viozzi, C.F.; Shivers, P.; Gellrich, N.C.; Powers, D.B. A New Hope: Patient-Specific Bone-Anchored Subperiosteal Implants: Perspective of 3 US Institutions on This Resurrected Treatment Modality. *J. Oral Maxillofac. Surg.* **2024**, *19*, 134–137. [CrossRef] [PubMed]

Disclaimer/Publisher's Note: The statements, opinions and data contained in all publications are solely those of the individual author(s) and contributor(s) and not of MDPI and/or the editor(s). MDPI and/or the editor(s) disclaim responsibility for any injury to people or property resulting from any ideas, methods, instructions or products referred to in the content.